Flow rate evaluation in parallel pump arrangements: Two case studies

J. Lanzersdorfer*† M. Schmidt* J. Pichler*

July 28, 2016

Abstract

Hydraulic tests on pumps for industrial applications pose several challenges for measurement engineers. Among them, conditions for pressure and flow rate measurement do usually not comply with standards for precision measurements. It is therefore common to perform factory acceptance tests to achieve high accuracy. In certain cases performance testing on site remains inevitable. In here, we present two case studies of off-factory measurements using index testing on parallel arranged pumps. The focus of these studies is on the flow rate determination which comprises the choice and application of an adequate measurement method, a flow rate *calibration strategy* and a reliability test of the results. It is finally possible to determine the weights of the measured branch flow rates. Comparisons with accessible performance data correlate very well and makes this kind of proceeding a powerful tool for volumetric discharge determination at unfavorable flow conditions.

*Andritz AG, Stattegger Strasse 18, 8045 Graz - Austria
†Corresponding author: johannes.lanzersdorfer@andritz.com

1 Introduction

The industry typically demands reliability of the production process and low power consumption from a pump, the efficiency is a minor matter. However, knowledge of the flow rate is of major interest for cooling water purposes. Cooling water circuits are mostly equipped with several parallel arranged pumps to avoid production losses and to adapt the number of operating pumps to the actual needs. The latter premises the knowledge of two subsequent facts to optimize the production process:

- the total flow rate and
- the flow proportion provided by an individual pump.

Pump testing at industrial facilities [1] challenges us since the structural requirements for proper measurement conditions are often inconsistent with financial aspects of the production. We therefore need to analyze the hydraulic, the metrological and the production related aspects of a test campaign in advance. As a result, we end up with a tailor-made *flow rate calibration strategy*, whose aim is to regress certain branch flow rates to available *index* parameters. The procedure of this strategy usually antecedes or goes along with the main measurements. In order to show the application of such flow rate calibrations we present two case studies of real test campaigns in the subsequent sections. In both cases single-path ultrasonic flowmeters in reflection mode were used which usually frown upon the turbine test community. However, the application of clamp-on acoustic flowmeters represents a cheap and – if you know how to use them – a reliable method for flow indication in the pump business.

The first case study gives insight into simultaneous measurements on five parallel arranged pumps which feed a refinery and neighboring industrial plants with cooling water. We present here the metrological and mathematical steps to determine the individual branch flow rates under – what test codes usually denote as – unfavorable measurement conditions.

The second study shows how the total flow rate in a cooling water system of a thermal power plant was determined by calibrating the flow rate measurements on three parallel system branches. Different *flow functions* are investigated towards statistical fitness and physical plausibility. We used this information to check and optimize the operating points in single-pump mode and dual-pump mode.

2 Case study: Determination of branch flows of five main cooling pumps without interrupting the production process

2.1 Description

In November 2015 we conducted a test campaign on the main cooling water circuit of a refinery, which is operated by OMV Deutschland GmbH, close to the town of Burghausen/Germany. There the refinery process plant and other neighboring industrial plants are continuously fed with cooling water by up to five parallel-driven vertical line shaft pumps (VLSPs). The power input per pump unit is approximately 1 MW, their service life and their hydraulic contour differ. The main target of the campaign was to evaluate the individual pump performance (i.e., Q-H-P) without interrupting the production process. Here, we focus on the flow rate evaluation of each pump branch.

Figure 1 shows a simplified P&ID. The VLSPs suck in water from an open basin and feed a collector pipe which provides cooling power to the individual consumers. Downstream the consumers the heated water is transmitted to the cooling tower where the thermal energy dissipates into the forced circulating air. Finally, the water drops back into the suction basin.

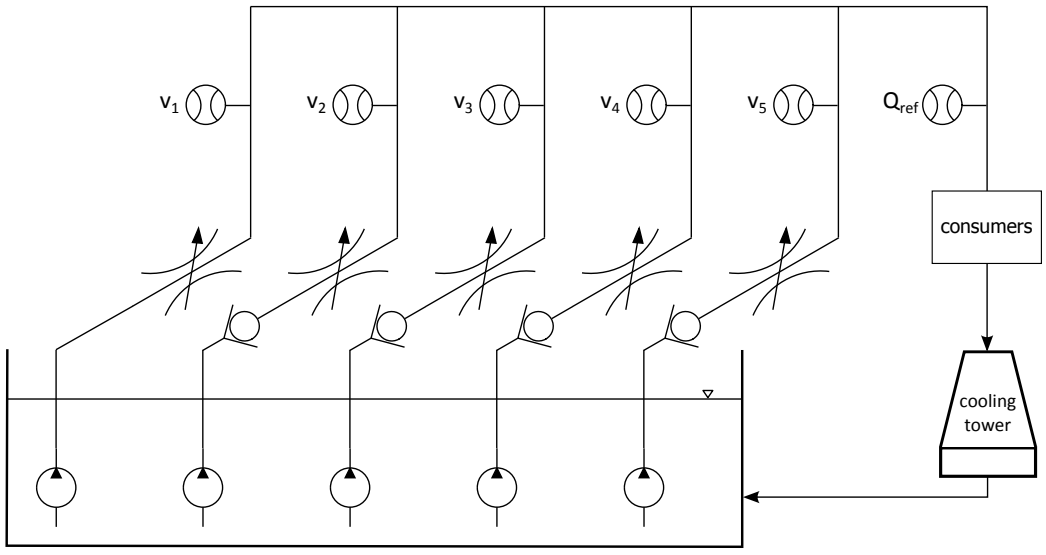

Figure 1: Simplified P&ID of the test setup on the main cooling water circuit at Burghausen refinery: Q_{ref} and v_i denote permanently and temporarily installed flow measurements, respectively.

The hydraulic conduit downstream the high-pressure flange of each VLSP is established by a horizontal part of $5D$ length, a 90° bend with $2D$ curvature radius, a vertical straight part with $10D$ length and another 90° bend leading to the horizontally aligned collector pipe. The initial, horizontal part comprises a swing type check valve (CV) – except for the pipe branch of pump #1 – followed by a manually operated butterfly valve (BV). There exists no adequate tappings for pressure measurements downstream the pump flange.

2.2 Test setup and procedure

Challenges and metrological strategy There is no general shutdown of the cooling circuit scheduled. The production lines need enough amount of cooling water with a minimum of three cooling pumps running. The application of an accurate, absolute flow measurement method on each pump branch would require an intervention into the production process, which stands without question. The additional costs for installations and modifications also made it less attractive for the client.

A combination of collector pipe flow measurement and secondary flow measurements on each branch as used for index tests [2] seemed to be best in line with the targets and the requirements. If possible the use of proper measurement of pressure losses along conduits represents a cheap and highly reliable method for flow indication. Unfortunately, there existed only few tappings which were poorly positioned next to hydraulic obstacles. We consequently decided to indicate the branch flow rates by means of the acoustic transit time method (ATTM) in single-path mode. We expected to adequately reduce the impact of the local cross flow on the velocity measurements in axial direction by arranging the sensor pairs in reflection mode. But the informative value of the measured velocity v remained questionable because of the presence of an axially asymmetric flow pattern. This was mainly caused by the upstream 90° bend. However, the normalized flow pattern at the acoustic measurement section was considered to be independent under changes of the branch flow rate as long as the hydraulic contour downstream the pump's high-pressure flange remained unchanged.[1] The axial velocity measured along an arbitrarily oriented[2] acoustic path is therefore always proportional to the real flow rate and a good estimate of the real branch flow

[1] For instance, the flow distribution is significantly disturbed by changing the opening angle of the BV.

[2] We disregard the trivial cases of path angles parallel and perpendicular to the pipe axis.

rate yields

$$Q_i = c_i \cdot A_i v_i \tag{1}$$

with the hydraulic cross section A_i and the unknown proportionality factor c_i. The total flow Q_{ref} can be calculated by summing up the proportions measured by the permanently installed devices (Venturi tube and orifice measurements).

Calibration strategy Since the water density at the measurement sections of the branch flow rates and of the permanent flowmeters does not alter significantly, the continuity equation simplifies to its volumetric representation and it yields

$$Q_{\text{ref}} \cong \sum_{i=1}^{5} Q_i \tag{2}$$

or

$$Q_{\text{ref}} \cong \sum_{i=1}^{5} c_i \cdot A_i v_i, \tag{3}$$

respectively (view Figure 2). The right side of equation (3) represents a model function – or simply called flow function – whose unknown coefficients have to be determined by linear regressing the *observations* Q_{ref} to the independent variables v_i. At least six[3] different operating points are required, where measurements of v_i's and Q_{ref} have to be taken, to check the statistical significance of the calculated coefficients c_i. There are three possibilities to change the operating conditions, which also can be used simultaneously:

1. Changing the flow resistance[4] downstream collector pipe, for instance, by opening/closing one or more valves along the production lines.

2. Changing the flow resistance of one or more pump branches by changing the BV opening.

3. Changing the combination of pump units under operation.

We wanted to avoid possibility 1 because the complex pipe branching at hand makes it almost impossible to eliminate any risk of failure indication

[3]The statistical degree of freedom need to be larger than zero:

$$d_{\text{f}} = n - m > 0$$

where n and m denote the number of observations and the number of regressors, respectively.

[4]More precisely: the dimensionless pressure loss coefficient ζ.

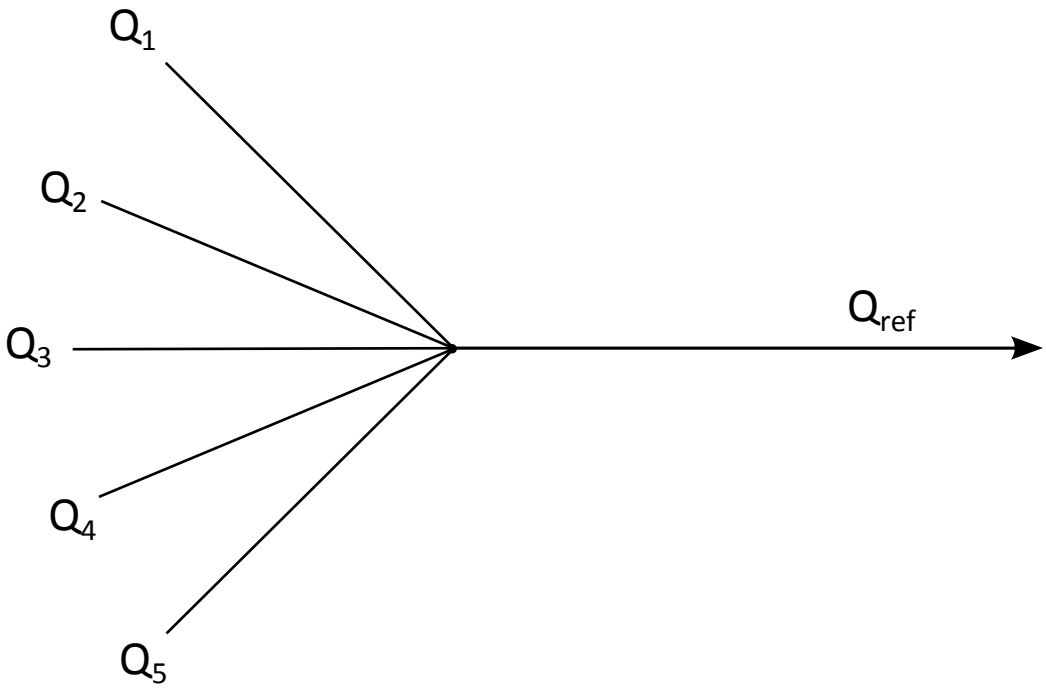

Figure 2: Flow diagram

in the subsequent production lines. The second possibility would strongly influence the flow pattern at the acoustic measurement section and, thus, the determination of the axial flow velocity v. The proportionality between flow estimate and measured axial velocity could not be established anymore. Finally, changing the number and choice of running pumps units remained the only degree of freedom to adjust the operating conditions. With the requirements of three units running at minimum, we obtain the maximum number of different operation points (= observations) by

$$n_{\max} = \sum_{k=3}^{5} \left(\begin{array}{c} n \\ k \end{array} \right) = 16 \quad . \tag{4}$$

That is, there are 1, 5 and 10 different pump combinations under five-units, four-units and three-units operation, respectively. With in total

$$d_{\mathrm{f}} = n_{\max} - m = 11$$

degrees of freedom we finally should end up with a low random uncertainty of the calibration coefficients c_i if the model function in (3) described the observed behavior well.

2.3 Test execution and results

On pump branch #4 we had to arrange the acoustic sensor pair in cater-cornered mode because of bad signal quality. Hence, one may expect additional terms in the flow rate estimate (1). For instance,

$$Q_4 = c_4 \cdot A_4 v_4 + g(v_4) \tag{5}$$

where $g(v_4)$ can represent some polynomial function of higher order. This deviation from an ideal behavior of a secondary flowmeter (i.e., Q/v =constant) does not downgrade the quality of the regression results as long as $d_\mathrm{f} \gg 0$.

In practice, we were only able to test the five-units operation and all combinations of the four-units operation, which gives a total number of $n = 6$ operating points. Three days of working in the open at rainy and cold days of November revealed us the limits of applicability of our ultrasonic flowmeters in use, which were 2 channel meter *Flexim Fluxus F601*, 2 channel meter *Siemens Sitrans FUP1010* and single channel meter *Panametrics PT878*. The first day of installation works was followed by another day of flow calibration measurements on five-units and four-units operation. Three-units operation was foreseen on the third day since the reduction of the cooling needs took approximately half a day. On day 3 only the Panametrics PT878 kept working under any combination of three-units operation, the other flowmeters obviously decided to go on strike. The reason of their breakdown is not clear to us but we suppose that the longterm application under adverse weather conditions were responsible to it. The low number of observations exclude the expansion of the model function (3) by any additional term as discussed in (5).

Table 1 shows the results of the flow measurements. Despite $d_\mathrm{f} = 1$ the random uncertainties of the regressors comprising a confidence interval of 95%, $e_\mathrm{r}(c_i)/c_i$, do not exceed ±0.4% (view Table 2). The sum of the calculated branch flows $\sum_i Q_i$ and the residuals $\sum_i Q_i - Q_\mathrm{ref}$ are given in Table 3. The residuals remain within ±0.01% which confirms the high significance of the chosen model function (3) with respect to Q_ref. The values in Table 2 deviate more or less from 1 for an ideal flow measurement. The largest correction has to applied on the measurement data of pump #4. There, the measured flow rate underestimated the calibrated flow estimate by approximately −7%. It was obvious that the asymmetric flow pattern impacts strongest on the axial velocity measurement of this branch's cater-cornered sensor positioning. The other measurements have to be corrected by values between −5.7% and +4.0% except for the measurement on pump #1. So,

there is no clear tendency in adjusting the values in positive or in negative direction. We installed the reflection mode arranged sensor pairs similarily in azimuthal and in longitudinal locations but we have used different types of sensors and flowmeters. Therefore, it is not possible to apportion the metrological quality among the test setup or the hydraulic flow behavior.

Let us take a closer look onto the results of pump #1. Taking account of the random uncertainty the flow measurement on this unit can be considered as *ideal* measurement. We actually had better metrological conditions on this unit compared to the setup on the other four units. The flange transitions are smooth at this unit, which made the head measurements more reliable. Pump #1 is smaller in geometry and the branch pipe has no CV. The nominal pipe lengths are longer which favors the inflow conditions into the acoustic measurement zone. Despite its age of more than 25 years no cavitation related abrasion damages were detected so far on the hydraulic contour [3]. This gives us the opportunity to compare our flow measurements with the factory acceptance test on this unit from 1990. Figure 3 clearly shows that the acceptance test curve could be reproduced well since the largest absolute deviation in head is only 0.5%.

We conclude that the calibration procedure of each branch flow velocity measurement v_i with respect to reference flow rate Q_{ref} was successful. A proof of the correctness of the reference flow rate by comparing it with an absolute flow measurement method is missing. However, the verification of the pump characteristics of pump #1 gives an indication for the validity of the reference flow. Within the flow rate interval $Q_i \in [0.6, 0.8] \cdot Q_{\text{rated}}$ the proportionality between axial velocity as measured and branch flow rate could be verfied with high significance. But outside this interval, the metrological behavior may differ and cannot be described by equation (1) anymore.

Table 1: Normalized measurement results

#	$\frac{A_1 v_1}{Q_{\text{rated}}}$	$\frac{A_2 v_2}{Q_{\text{rated}}}$	$\frac{A_3 v_3}{Q_{\text{rated}}}$	$\frac{A_4 v_4}{Q_{\text{rated}}}$	$\frac{A_5 v_5}{Q_{\text{rated}}}$	$\frac{Q_{\text{ref}}}{Q_{\text{rated}}}$
-	-	-	-	-	-	-
1	0.00009	0.91725	0.97508	0.93403	0.99999	3.84716
2	0.59551	0.79763	0.89294	0.83381	0.89647	4.03405
3	0.79319	0.00022	1.00248	0.95711	1.03134	3.76891
4	0.79986	0.93167	0.00011	0.94415	1.03239	3.75389
5	0.80366	0.93415	1.01346	0.00149	1.04005	3.74787
6	0.79981	0.92718	0.99244	0.95106	0.00033	3.75090

Table 2: Results of the regression analysis ($d_{\text{f}} = 1$, confidence interval 95%)

parameter	unit	value ± random uncertainty
c_1	-	1.002 ± 0.004
c_2	-	1.040 ± 0.003
c_3	-	0.975 ± 0.003
c_4	-	1.069 ± 0.003
c_5	-	0.943 ± 0.003

Table 3: Comparison of reference and regression flow rate

#	$\frac{Q_{\text{ref}}}{Q_{\text{rated}}}$	$\frac{\sum_i Q_i}{Q_{\text{rated}}}$	residual
-	-	-	-
1	3.84716	3.84709	-0.00007
2	4.03405	4.03428	0.00023
3	3.76891	3.76887	-0.00005
4	3.75389	3.75386	-0.00004
5	3.74787	3.74782	-0.00004
6	3.75090	3.75086	-0.00004

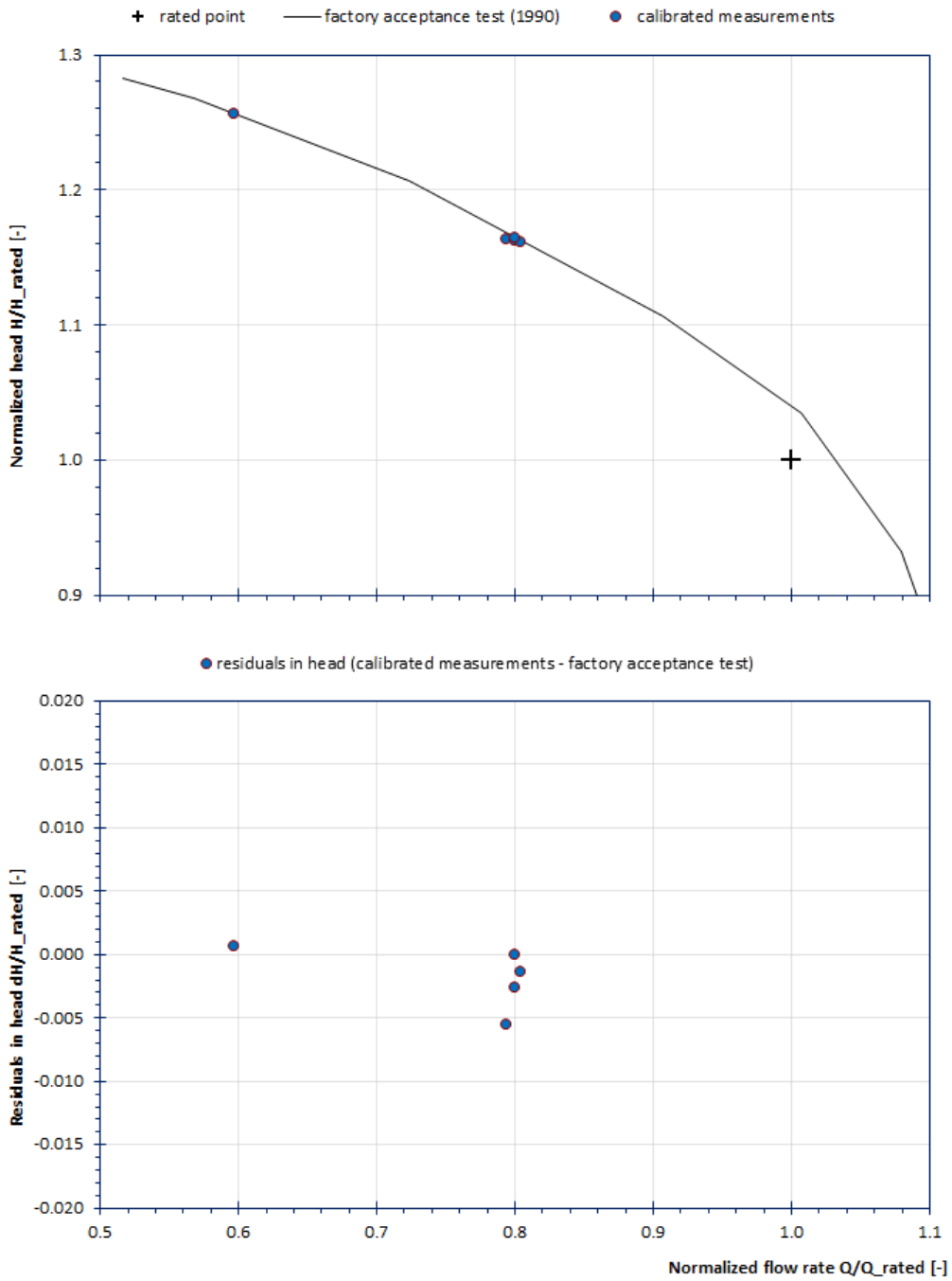

Figure 3: Pump #1: Comparison of the branch-flow-calibrated performance test (circle) with the original factory acceptance test data from 1990 (line). Measurement data are speed-converted.

3 Case study: Optimization of pump operation points on main cooling circuit

3.1 Description

In April 2016 the Knippegroen gas power plant, which is located close to Ghent/Belgium, was subject of general revision works. During the down time of the power generation unit the operating points of the two main cooling pumps should be checked and – if necessary – it should be optimized for single-pump mode and for dual-pump mode. Referring to the P&ID in Figure 4 cooling water is stored below the cooling tower in an open basin. Two parallel arranged VLSPs pump the water into the subterranean, *cold* collector pipe leading to the power house. There, the collector pipe subdivides into two major pipes, which feed the condenser to cool the water of the primary circuit, and a minor pipe providing cooling power to auxiliary devices. All three branches unite subsequently in the *hot* collector pipe situated underground. It leads back to the cooling tower, where the water temperature is reduced by forced air-conditioning. The pumps require approximately 1 MW of electrical power each. Both have identical hydraulic contours.

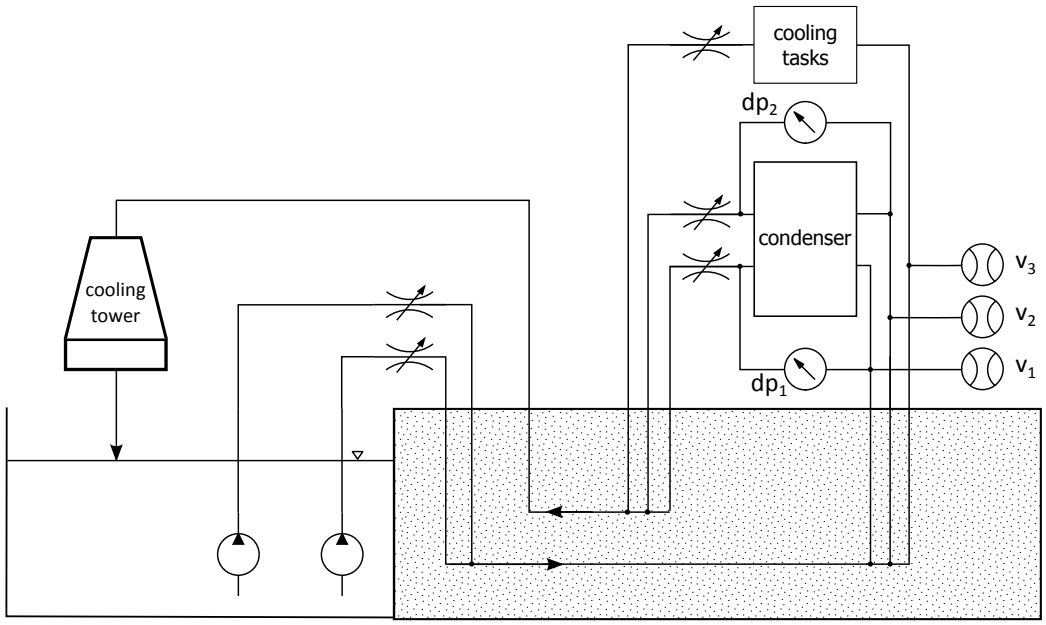

Figure 4: Simplified P&ID of the test setup on the main cooling water circuit at Knippegroen gas power plant: v_i denote the temporarily installed flow velocity measurements, Δp_i are the permanently installed pressure devices.

3.2 Test setup and procedure

Challenges and metrological strategy The pipings of the cooling circuit is made of glass-fiber reinforced plastic (GRP) except those parts used for direct heat-exchange. The automatic-operated BV downstream the high-pressure pump flange is not designed for throttle purposes but only for starting and stopping the pump. There is no possibility in installing an acoustic clamp-on flowmeter onto the pump branch anywhere between high-pressure flange and the conjunction with the subterranean collector pipe. The accessible pipeworks outside and inside the powerhouse is very complex. A few pressure tappings are available, but their positionings and the asymmetric flow pattern give rise to distrust of the measurement quality. The two BVs downstream the condenser are fully opened at dual-pump mode and partly opened at single-pump mode. The cooling branch for auxiliary tasks is never throttled under normal plant operation.

There exists permanent measurement devices for the pressure losses of each condenser branch, Δp_1 and Δp_2, which can be used to indicate the flow rate Q_1 and Q_2, respectively. The quality of theses measurements was unknown beforehand. Therefore, we decided to record these pressures for backup reasons but ATTM should be used as primary flow indication. We chose measurement sections upstream the condenser or any cooling task for the axial flow velocity measurements. On each branch pipe an ultrasonic sensor pair was mounted in reflection mode. Here again, we made a simplified assumption that the normalized flow pattern at the measurement sections remain independent from the flow rate. And we avoid any unpredictable impact onto the velocity distribution by flow throttling at the manually op-

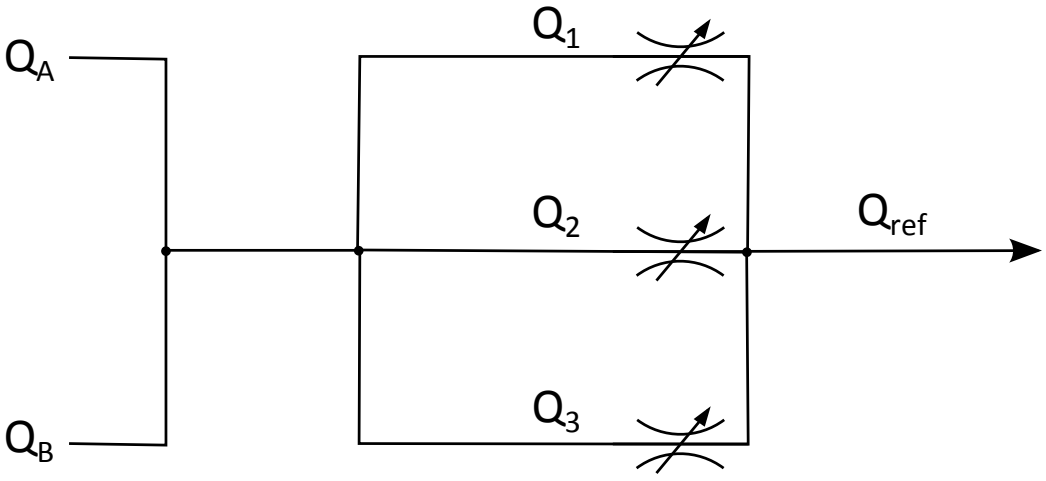

Figure 5: Flow diagram

erated BVs far downstream. Figure 5 shows a simplified representation of the cooling water flow. The down time of the power generating unit offered additional possibilities in operating the cooling circuit. The auxiliary branch and at maximum one of the major branches could have been put out of service if desired. Anyhow, we did not want to perform any tests on operating conditions for which the cooling water circuit maybe has not been designed. The calibration tests were partly done with a closed auxiliary pipe.

Calibration strategy Since it is impossible to measure any reference flow rate in the underground collector pipe we cannot proceed with the branch flow calibration as described in the previous case study. We need to subdivide our calibration routine into three steps:

1. We keep one pump unit running under stable conditions and maintain a constant static pump head H_{st} by adjusting the openings of the BVs downstream the acoustic measurement sections. Neglecting any excessive change of the fluid viscosity the stable pressure head guarantees a constant volumetric flow rate. We set this unknown total flow rate $Q_{\mathrm{ref}} = Q_{\mathrm{rated}}$ because – at this state – there is no need for the correct value. The continuity law under constant density yields

$$f_i \cong Q_{\mathrm{ref}} = Q_{\mathrm{rated}} \tag{6}$$

with the model functions of the flow f_i, which are introduced subsequently.
As described in the previous subsection there are several possibilities in indicating the branch flow rates by clamp-on flowmeters and by measurements of pressure losses. Primarily, we use the acoustic measurements on all three branches, yielding the model function

$$f_1 = \sum_{i=1}^{3} c_{1i} \cdot A_i v_i. \tag{7}$$

We assume discharge-independent, normalized velocity profiles at all measurement sections with cross-section A_i. Together with the sensor arrangements in reflection mode the simple representation of (7) is reasonable. Using the pressure loss parameters Δp_1 and Δp_2 and assuming $(Q_i)^2$-dependency, we alternatively may define

$$f_2 = \sum_{i=1}^{2} c_{2i} \cdot \left(\frac{\Delta p_i}{1\ \mathrm{bar}} \right)^{0.5} + c_{23} \cdot A_3 v_3. \tag{8}$$

Finally, a more general representation of (8)

$$f_3 = \sum_{i=1}^{2} c_{3i} \cdot \left(\frac{\Delta p_i}{1 \text{ bar}} \right)^{n_i} + c_{33} \cdot A_3 v_3, \tag{9}$$

is investigated in addition to (7) and (8). These three definitions are most probable and physically relevant. Other flow functions are not discussed in this paper.
The number of regressors m equals 3 and 5 for the model functions (7)–(8) and 9, respectively. We hence need at least $n = 6$ calibration measurements to evaluate all model functions statistically.

2. Here, the missing proportionality factor between the scaled model test flow and the calibrated flow has to determined. Additionally, a plausibility check of the model function is done within the normal operating range in single-pump mode. For this, an index test on a single pump unit is executed. Comparing the measured pump characteristics with scaled model test data under assimilable NPSH values yields the proportionality coefficient

$$k_i = \frac{Q_{\text{model}}}{f_i}. \tag{10}$$

Depending on the choice of the model function we obtain the total flow rate by

$$Q = k_i \cdot f_i = \sum_{j=1}^{3} Q_{ij}, \tag{11}$$

where the indices i and j denote the choice of the model function (7)–(9) and the branch identification number, respectively. The flow rates through the condenser branches ($j \in \{1, 2\}$) may consequently estimated by

$$Q_{1j} = k_1 \cdot c_{1j} \cdot A_j v_j, \tag{12}$$

$$Q_{2j} = k_2 \cdot c_{2j} \cdot \left(\frac{\Delta p_j}{1 \text{ bar}} \right)^{0.5} \quad \text{or} \tag{13}$$

$$Q_{3j} = k_3 \cdot c_{3j} \cdot \left(\frac{\Delta p_j}{1 \text{ bar}} \right)^{n_j}. \tag{14}$$

The discharge estimates flowing through the auxiliary pipe yields

$$Q_{j3} = k_j \cdot c_{j3} \cdot A_3 v_3 \qquad \forall j \in \{1, 2, 3\}. \tag{15}$$

We check the plausibility of each model function within the tested range in single-pump mode by comparing the *calibrated* $Q-H$-characterstics with the scaled model test data. If position and/or orientation of the curves differed clearly the model function should be discarded. Finally, the characteristics of the other unit in single-pump mode has to be determined using calibration data of a plausible flow function.

3. The reliability of each model function needs to be tested by using measurement data in dual-pump mode. We compare here the total flow rate (11) with the sum of the individual pump flow rates. The latter are obtained by interpolating the corresponding index test data $Q(H_{\mathrm{st}})$, which were provided in the previous enumeration point. The absolute magnitude of the difference

$$\Delta Q = Q - Q[(H_{\mathrm{st}})_{\mathrm{A}}] - Q[(H_{\mathrm{st}})_{\mathrm{B}}] \tag{16}$$

from zero is a measure of reliability at high flow rates of the model function under investigation.

3.3 Test execution and results

We equipped both main pipes upstream the condenser entrance with clamp-on sensor pairs of same type in reflection mode arrangement. A 2-channel meter *Siemens Sitrans FUP1010* provided the axial flow velocity data. A different pair of sensors in reflection mode was fitted onto the auxiliary pipe and a *Flexim Fluxus F601* flowmeter provided the axial flow velocity data.

Determination of the model function coefficients Step #1 of the calibration procedure was executed with pump A in single-pump operation. We changed the openings of two BVs downstream the heat exchangers arbitrarily and tuned the third one to get the same static head at all these measuring points. We recorded the parameters v_1, v_2, v_3, Δp_1, Δp_2 and $(H_{\mathrm{st}})_{\mathrm{A}}$ with $n = 9$ different BV openings. The static heads could be kept constant within $\pm 0.20\%$, which ensures almost identical total flow rates. The measurement data are given in Table 4, the regression results follow in Tables 5-6 and in Figure 6.

The residuals remain within $[-0.57\%, 0.29\%]$ but scatter most for model function f_1, which exclusively uses the acoustic velocity measurements. Minimal dispersion is obtained with model function f_3 (i.e., $[-0.07\%, 0.11\%]$), but the random uncertainty of the corresponding regressors exceeds the expectations (see Table 5). The residuals of f_2 scatter slightly more than those of f_3.

Table 4: Normalized measurement results of calibration step #1

#	$\frac{A_1 v_1}{Q_{\text{rated}}}$	$\frac{A_2 v_2}{Q_{\text{rated}}}$	$\frac{A_3 v_3}{Q_{\text{rated}}}$	Δp_1	Δp_2	$\frac{(H_{\text{st}})_{\text{A}}}{H_{\text{rated}}}$
-	-	-	-	bar	bar	-
1	0.5458	0.5563	-0.0002	0.3044	0.2816	0.7800
2	0.4862	0.6087	-0.0001	0.3650	0.2276	0.7796
3	0.4272	0.6581	-0.0001	0.4270	0.1801	0.7798
4	0.6160	0.4850	-0.0005	0.2396	0.3552	0.7787
5	0.6959	0.4213	0.0000	0.1819	0.4375	0.7800
6	0.5088	0.5291	0.0545	0.2827	0.2549	0.7792
7	0.5940	0.4603	0.0545	0.2140	0.3316	0.7789
8	0.5297	0.4614	0.1094	0.2128	0.2771	0.7800
9	0.4743	0.5110	0.1107	0.2615	0.2252	0.7811

Table 5: Results of the regression analyses of model functions (7)–(9) (confidence interval 95%)

parameter	unit	value ± random uncertainty
c_{11}	-	0.857 ± 0.021
c_{12}	-	0.962 ± 0.021
c_{13}	-	0.929 ± 0.063
c_{21}	m^3/s	0.942 ± 0.006
c_{22}	m^3/s	0.904 ± 0.006
c_{23}	-	0.806 ± 0.016
c_{31}	m^3/s	0.905 ± 0.214
n_1	-	0.578 ± 0.213
c_{32}	m^3/s	0.956 ± 0.194
n_2	-	0.444 ± 0.118
c_{33}	-	0.812 ± 0.136

Table 6: Comparison of reference and regression flow rates

#	$\frac{Q_{\text{ref}}}{Q_{\text{rated}}}$	$\frac{f_1}{Q_{\text{rated}}}$	$\frac{f_2}{Q_{\text{rated}}}$	$\frac{f_3}{Q_{\text{rated}}}$	residual_1	residual_2	residual_3
-	-	-	-	-	-	-	-
1	1.0000	1.0029	0.9995	0.9993	0.0029	-0.0005	-0.0007
2	1.0000	1.0023	1.0005	1.0006	0.0023	0.0005	0.0006
3	1.0000	0.9993	0.9993	0.9997	-0.0007	-0.0007	-0.0003
4	1.0000	0.9943	0.9997	0.9994	-0.0057	-0.0003	-0.0006
5	1.0000	1.0019	1.0000	1.0000	0.0019	0.0000	0.0000
6	1.0000	0.9958	1.0014	1.0011	-0.0042	0.0014	0.0011
7	1.0000	1.0027	1.0005	1.0008	0.0027	0.0005	0.0008
8	1.0000	0.9996	0.9989	0.9994	-0.0004	-0.0011	-0.0006
9	1.0000	1.0011	1.0002	0.9996	0.0011	0.0002	-0.0004

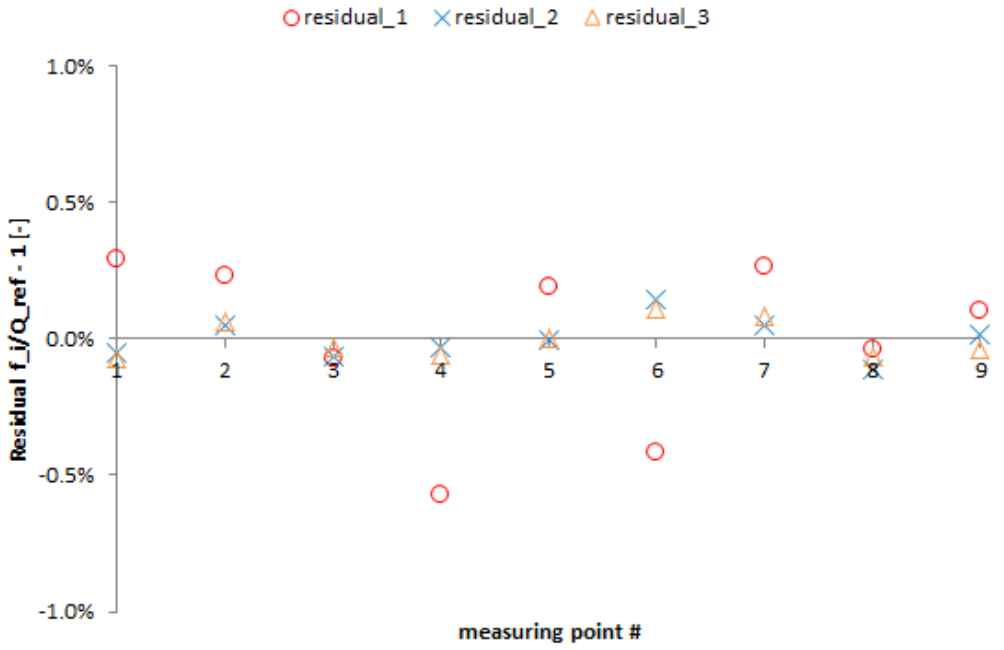

Figure 6: Residuals of the model functions f_1 (circle), f_2 (cross) and f_3 (triangle) compared to the reference flow

However, it has the lowermost standard deviation owing to $(d_\mathrm{f})_{f_2} - (d_\mathrm{f})_{f_3} = 2$. This indicates, that the determination of the exponents n_1 and n_2 does not provide any gain in accuracy. Its regressors c_{2j} have lower random uncertainties than c_{1j}. This can be explained by the low dispersion behavior of typical pressure measurements compared to ATTM. It is worth mentioning that the weight of auxiliary flow rate as measured, c_{i3}, which should be independent of the choice of model function differs significantly in f_1 compared to the others. Whereas $c_{23} \cong c_{33} \cong 0.81$, the exclusive usage of ATTM in model function f_1 weights the auxiliary flow rate by $c_{13} \cong 0.93$. This large deviation creates doubts in the power of explaining the flow behavior by f_1 or by $f_2(f_3)$ or by the three model functions at all.

Index test and reliability in single-pump mode The BV of the auxiliary branch was completely opened, which represents the default state during plant operation. For index testing the flap position of the condenser pipe valves were adjusted in the same manner to feed the main branches almost equally. First, we recorded the pump characteristics of pump A. Then the

calibration coefficient k_i can be determined, for instance, by minimizing

$$\min \left\{ \sum_{j=1}^{n} \left[k_i \cdot f_i(j) - Q_{\mathrm{smt}}(H_{\mathrm{st}}(j)) \right]^2 \right\}. \tag{17}$$

The parameter $Q_{\mathrm{smt}}(H_{\mathrm{st}}(j))$ denotes the pump flow rate based on the scaled model test data as a function of the measured static head. We recorded in total $n = 10$ different operating points. In any case, the measurement data require speed-conversion for every comparison with model test data. Figure 7 shows the static head as a function of pump flow rate as expected by model testing and as measured, calibrated by flow function f_i and adjusted by k_i. The minimum of (17) is obtained independently of the chosen function f_i by almost the same proportionality factor. This would be expectable if all flow functions scaled linearly with the real flow rate. The scaling factor yields

$$k_1 \cong k_2 \cong k_3 = k = 1.147 \pm 2\% \tag{18}$$

The assigned uncertainty of $\pm 2\%$ is based on experience and takes into consideration the credibility of the model test scaling for pump types of that specific speed. The individual curves give confidence in relying on all three flow functions f_i within the operating range in single-pump mode. Unfortunately, the current status does not allow us to explain the deviation $c_{13} \neq c_{23} \cong c_{33}$ stated previously.

Reliability in dual-pump mode For this purpose both main pumps were operated parallel and the parameters v_1, v_2, v_3, Δp_1, Δp_2, $(H_{\mathrm{st}})_{\mathrm{A}}$ and $(H_{\mathrm{st}})_{\mathrm{B}}$ were recorded at three different circuit characteristics. We calculate the total flow rate by means of the flow function f_i to be tested and it yields

$$Q = k \cdot f_i(v_1, v_2, v_3, \Delta p_1, \Delta p_2) \tag{19}$$

The proportion of each pump is obtained by interpolating the already available index test data. The sum of both pump flow rates is consequently subtracted from (19) to obtain the residual ΔQ. Tables 7–9 reveal the corresponding results of the three measured operating conditions at dual-pump mode. We recognize that both flow functions using the permanent pressure parameters, i.e., f_2 and f_3, explicitly fail in describing the flow behavior beyond the operating range of a single pump. We face deviations of approximately 6%. It could be shown that each measured pressure difference does not scale with the squared branch flow rate, which can be attributed to inadequate positioning of one or both pressure measurement sections along each

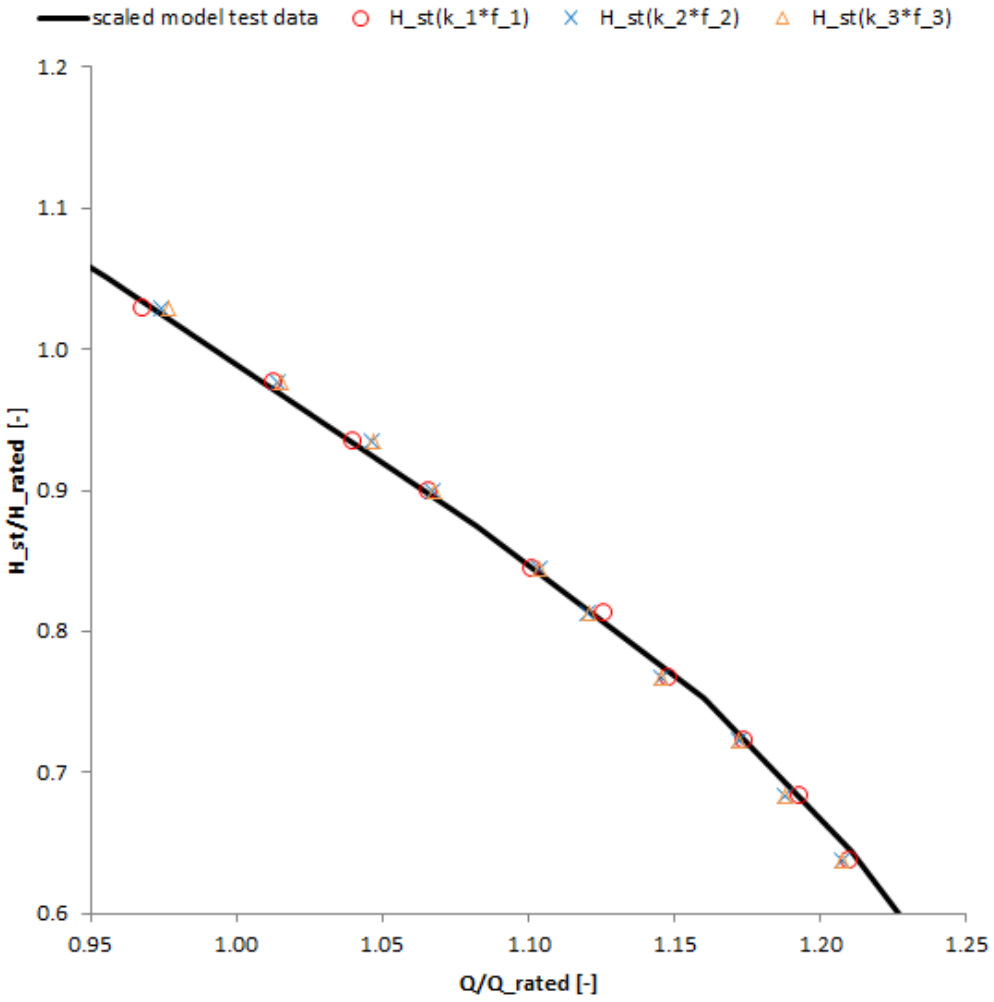

Figure 7: Comparison of scaled model test data (line) with measured pump-characteristics using the flow rate definitions of $k_1 \cdot f_1$ (circle), $k_2 \cdot f_2$ (cross) and $k_3 \cdot f_3$ (triangle). Measurement data are speed-converted.

condenser branch. On the other hand the linearity of f_1 could be demonstrated very well showing residuals within $\pm 0.50\% \cdot \{Q[(H_{\mathrm{st}})_{\mathrm{A}}] + Q[(H_{\mathrm{st}})_{\mathrm{B}}]\}$. That is, only the reliability of f_1 using calibrated three, single-path ATTM in reflection mode could be confirmed and the regressor c_{13} seems to be trustworthy. The coefficients $c_{23} \cong c_{33}$ are identified as doubtful. We finally calculate the total flow rate (11) with Table 5 and equation (18) by

$$Q = \kappa_1 \cdot A_1 v_1 + \kappa_2 \cdot A_2 v_2 + \kappa_3 \cdot A_3 v_3. \tag{20}$$

The coefficients $\kappa_i = k \cdot c_{1i}$ are given in Table 10. The results show that the

measured flow rate in condenser pipe 1 is almost identical to the calibrated flow but the measured condenser pipe flow 2 is considerably underestimated by -10%. The measurements on the auxiliary pipe is underestimated from a subjective point of view taking into account the higher relative uncertainty.

Table 7: Reliability of flow function f_1 in dual-pump mode

#	$\frac{Q}{Q_{\text{rated}}}$	$\frac{Q_{\text{A}}+Q_{\text{B}}}{Q_{\text{rated}}}$	$\frac{\Delta Q}{Q_{\text{rated}}}$
-	-	-	-
1	2.081	2.071	0.010
2	2.031	2.034	-0.002
3	1.981	1.989	-0.008

Table 8: Reliability of flow function f_2 in dual-pump mode

#	$\frac{Q}{Q_{\text{rated}}}$	$\frac{Q_{\text{A}}+Q_{\text{B}}}{Q_{\text{rated}}}$	residual
-	-	-	-
1	1.938	2.068	-0.130
2	1.900	2.027	-0.127
3	1.862	1.982	-0.120

Table 9: Reliability of flow function f_3 in dual-pump mode

#	$\frac{Q}{Q_{\text{rated}}}$	$\frac{Q_{\text{A}}+Q_{\text{B}}}{Q_{\text{rated}}}$	residual
-	-	-	-
1	1.951	2.068	-0.117
2	1.912	2.028	-0.115
3	1.872	1.983	-0.111

Table 10: Coefficients of total flow function (20)

parameter	unit	value $\pm$ uncertainty
κ_1	-	0.983 ± 0.031
κ_2	-	1.104 ± 0.030
κ_3	-	1.065 ± 0.070

4 Conclusion

We described how to implement tailor-made calibration procedures successfully on multi-branch flow measurements. They offer possibilities to combine different methods of flow indication such as ATTM, pressure losses or Winter-Kennedy differential pressure and to weigh their influence on the total discharge adequately.

A single-path ATTM setup in reflection arrangement could be verified as a reliable tool for discharge indication even under unfavorable measurement conditions. However, the measurement quality depends mainly on the independence of the normalized velocity profile on the flow rate. Changing the hydraulic contour immediately upstream the acoustic measurement section disturbs the linearity between measured axial velocity and real flow rate.

We could successfully use pressure loss measurements together with branch flow calibrations to describe the flow behavior in the typical operating range of a single cooling pump. But the choice of flow function failed in dual-pump mode which could be traced back to the improper positioning of the tappings and the asymmetric velocity profiles at hand.

Used symbols and abbreviations

Symbol	Description	Unit
A	hydraulic cross-section of the pipe	(m^2)
c	calibration factor	(-, m^3/s)
D	reference pipe diameter	(m)
f	model function of the reference flow rate	(m^3/s)
d_f	statistical degrees of freedom	(-)
H	total pump head	(m)
H_{rated}	rated pump head	(m)
H_{st}	static pump head	(m)
k	calibration factor	(-)
m	number of regressors	(-)
n	number of observations	(-)
n	calibration exponent	(-)
Q	calibrated branch flow rate	(m^3/s)
Q_{rated}	rated flow rate	(m^3/s)
Q_{ref}	reference flow rate	(m^3/s)
v	axial velocity as measured	(m/s)
Δp	Pressure losses as measured	(Pa)
κ	calibration factor	(-)
ρ	Water density	(kg/m^3)

Abbreviation	Description
ATTM	acoustic transit time method
BV	butterfly valve
CV	swing type check valve
VLSP	vertical line shaft pump

References

[1] ISO, editor. *ISO 9906 – Rotodynamic pumps – Hydraulic performance acceptance tests – Grades 1, 2 and 3.* ISO, 2 edition, 2012.

[2] IEC, editor. *IEC 60041 – Field acceptance tests to determine the hydraulic performance of hydraulic turbines, storage pumps and pump-turbines.* IEC, 3 edition, 1991.

[3] Information provided by OMV Deutschland GmbH.